

14. **Enomoto A, Kimura H, Chairoungdua A, Shigeta Y, Jutabha P, Cha SH, Hosoyamada M, Takeda M, Sekine T, Igarashi T, Matsuo H, Kikuchi Y, Oda T, Ichida K, Hosoya T, Shimokata K, Niwa T, Kanai Y, Endou H** 2002 Molecular identification of a renal urate anion exchanger that regulates blood urate levels. *Nature* 417:447-452
15. **Ichida K, Hosoyamada M, Hisatome I, Enomoto A, Hikita M, Endou H, Hosoya T** 2004 Clinical and Molecular Analysis of Patients with Renal Hypouricemia in Japan-Influence of URAT1 Gene on Urinary Urate Excretion. *Journal of the American Society of Nephrology* 15:164-173
16. **Komoda F, Sekine T, Inatomi J, Enomoto A, Endou H, Ota T, Matsuyama T, Ogata T, Ikeda M, Awazu M, Muroya K, Kamimaki I, Igarashi T** 2004 The W258X mutation in SLC22A12 is the predominant cause of Japanese renal hypouricemia. *Pediatr Nephrol* 19:728-733
17. **Kikuchi Y, Koga H, Yasutomo Y, Kawabata Y, Shimizu E, Naruse M, Kiyama S, Nonoguchi H, Tomita K, Sasatomi Y, Takebayashi S** 2000 Patients with renal hypouricemia with exercise-induced acute renal failure and chronic renal dysfunction. *Clin Nephrol* 53:467-472
18. **Tazawa M, Morooka M, Takeichi S, Minowa S, Yasaki T** 1996 Exercise-induced acute renal failure observed in a boy with idiopathic renal hypouricemia caused by postsecretory reabsorption defect of uric acid. *Jpn J Nephrol* 38:407-412

Diabetologia Clinical and Experimental Diabetes and Metabolism
© Springer-Verlag 2005
10.1007/s00125-004-1646-6

Article

Renal clearance of glycolaldehyde- and methylglyoxal-modified proteins in mice is mediated by mesangial cells through a class A scavenger receptor (SR-A)

K. Nakajou¹, S. Horiuchi² , M. Sakai², N. Haraguchi¹, M. Tanaka³, M. Takeya³ and M. Otagiri¹

(1)^{*} Department of Biopharmaceutics, Graduate School of Pharmaceutical Sciences, Kumamoto University, Kumamoto, Japan

(2)^{*} Department of Medical Biochemistry, Graduate School of Medical Sciences, Kumamoto University, 1-1-1 Honjo, Kumamoto 860-0811, Japan

(3)^{*} Department of Cell Pathology, Graduate School of Medical Sciences, Kumamoto University, Kumamoto, Japan

 S. Horiuchi

Email: horouchi@gpo.kumamoto-u.ac.jp

Phone: +81-96-3735070

Fax: +81-96-3646940

Received: 11 June 2004 / Accepted: 22 October 2004 / Published online: 15 January 2005

Abstract

Aims/hypothesis Glomerular mesangial expansion is a characteristic feature of diabetic nephropathy, and the accumulation of AGE in the mesangial lesion has been implicated as one of its potential causes. However, the route for the AGE accumulation in mesangial lesions in diabetic patients is poorly established.

Methods Glycolaldehyde-modified BSA (GA-BSA) and methylglyoxal-modified BSA (MG-BSA) were prepared as model AGE proteins, and their in vivo plasma clearance was examined in mice, and renal uptake by in vitro studies with isolated renal mesangial cells.

Results Both ¹¹¹In-GA-BSA and ¹¹¹In-MG-BSA were rapidly cleared from the circulation mainly by both the liver and kidney. Immunohistochemical studies with an anti-GA-BSA antibody demonstrated that intravenously injected GA-BSA accumulated in mesangial cells, suggesting that such cells play an important role in the renal clearance of circulating AGE proteins. Binding experiments at 4°C using mesangial cells isolated from mice showed that ¹²⁵I-GA-BSA and ¹²⁵I-MG-BSA exhibited specific and saturable binding. Upon incubation at 37°C, ¹²⁵I-GA-BSA and ¹²⁵I-MG-BSA underwent endocytic degradation by these cells. The binding of the ligands to these cells was inhibited by several ligands for scavenger receptors. The endocytic degradation of GA-BSA by mesangial cells from class A scavenger receptor (SR-A) knock-out mice was reduced by 80% when compared with that of wild-type cells. The glomerular accumulation of GA-BSA after its intravenous administration was attenuated in SR-A knock-out mice, as evidenced by immunohistochemical observations.

Conclusions/interpretation These results raise the possibility that circulating AGE-modified proteins are subjected to renal clearance by mesangial cells, mainly via SR-A. This pathway may contribute to the pathogenesis of AGE-induced diabetic nephropathy.

Keywords AGE - Biological fate - Diabetic nephropathy - Endocytosis - Intermediate aldehydes - Scavenger receptor

Abbreviations *Ac-LDL* Acetylated LDL - *GA* Glycolaldehyde - *MG* Methylglyoxal - *Ox-LDL* Oxidized LDL - *SR-A* Class A scavenger receptor

Introduction

The long-term incubation of proteins with glucose leads, through the formation of early products such as Schiff bases and Amadori products, finally to AGE. AGE proteins are characterised physicochemically by their fluorescent, brown color and intramolecular and intermolecular cross-linking [1], and biologically by their recognition by specific AGE receptors [2]. Recent studies reported that several aldehydes such as glycolaldehyde (GA), glyoxal, methylglyoxal (MG), and 3-deoxyglucosone are generated during the Maillard reaction from glucose, a Schiff base, or Amadori products [3, 4]. A much stronger chemical reactivity than that of glucose indicates the important role of these aldehydes in the in vivo generation of AGE structures [5-7].

Previous studies have provided several lines of evidence for the pathological role of AGE in diabetic nephropathy. First,

immunological studies using an anti-AGE antibody demonstrated the accumulation of AGE in glomerular mesangial lesions of diabetic nephropathy [8, 9]. Second, AGE proteins prepared by the modification of BSA with ribose, induced TGF- β synthesis at an mRNA level in rat mesangial cells [10]. Third, AGE proteins prepared by incubating BSA with glucose-6-phosphate increased the levels of growth factors such as TGF- β and IGF-I and extracellular matrix proteins such as fibronectin, laminin and type IV collagen at the protein level in rat mesangial cells [11, 12]. Fourth, AGE proteins prepared by incubating BSA with glucose-6-phosphate also increased type IV collagen expression in human mesangial cells [13]. Finally, AGE proteins prepared by incubating BSA with glucose, glyceraldehyde, or GA induced the production of vascular endothelial growth factor and monocyte chemoattractant protein-1 in human mesangial cells [14].

These cellular responses to AGE proteins are believed to be mediated by AGE receptors which include the receptor for AGE (RAGE) [15], oligosaccharyltransferase-48 (OST-48), 80K-H, galectin-3 complex [16], and scavenger receptors such as the class A scavenger receptor (SR-A) [17], CD36 [18], SR-BI [19], and LOX-1 [20]. Several AGE receptor(s) in mesangial cells were characterised from the potential link to diabetic nephropathy [21–23]. However, one important issue that remains unknown concerns the access of AGE ligands to these AGE receptors in the mesangial area. More specifically, it is important to determine whether AGE proteins that accumulate in the mesangium are produced at the same site, or are produced in other places and then delivered to the mesangial area. We hypothesised that the increased levels of plasma AGE proteins in the diabetic states are subjected to renal clearance by an active cellular process(es) which may lead to the subsequent accumulation of AGE proteins in the mesangial area and induction of biological responses by interacting with AGE receptors of mesangial cells. In the present study, GA-modified BSA (GA-BSA) and MG-modified BSA (MG-BSA) were prepared as model AGE proteins and their plasma and renal clearance examined in mice. The endocytic uptake of these AGE proteins by mesangial cells separated from SR-A knock-out mice was also compared with that of control mice.

Materials and methods

Chemicals BSA (fraction V) was purchased from Wako Pure Chemical Industries (Osaka, Japan). Penicillin G and streptomycin were purchased from Life Technologies (New York, NY, USA). RPMI 1640 medium, DMEM, Hanks' balanced salt solution (HBSS), biotinamidohexanoic acid *N*-hydroxysuccinimido ester (BNHS) and collagenase were obtained from Sigma Chemical (St Louis, MO, USA). ITS premix was obtained from Becton Dickinson (Bedford, MA, USA). Indium 111 trichloride (74 MBq/ml in 0.02 mol/l HCl) was a gift from Nihon Medi-Physics (Takarazuka, Japan), and Na¹²⁵I (3.7 GBq/ml in NaOH) was purchased from Amersham Pharmacia Biotech (Little Chalfont, Bucks, UK). All reagents used were of the highest grade available from commercial sources.

Animals Male ddY (27–32 g) and C57BL/6 (22–25 g) mice were obtained from SLC (Shizuoka, Japan). The mice were kept under a 12/12 h light/dark cycle in a humidity-controlled room.

Mice lacking both SR-A were established from C57BL/6 by the targeted disruption of exon 4 of the type AI/type AII SR gene, which is essential for the formation of functional trimeric receptors in A3-1 embryonic stem cells. Descriptions of the construct and the phenotypic expression in homozygous knock-out mice have been reported previously [24]. Normal littermates were bred as controls.

Ligand preparation To prepare GA-BSA, 5 mg/ml BSA was incubated with 50 mmol/l of GA at 37°C for 3 days in PBS, followed by dialysis against PBS [3]. MG-BSA was prepared under identical conditions except that 50 mmol/l carbonate buffer (pH 9.0) was used instead of PBS. LDL ($d=1.019\text{--}1.063$ g/ml) was isolated by the sequential ultracentrifugation of fresh plasma from normolipidaemic subjects after overnight fasting, and dialysed against 0.15 mol/l NaCl per 1 mmol/l EDTA (pH 7.4) [25]. Acetylated LDL (Ac-LDL) was prepared by the chemical modification of LDL with acetic anhydride as described previously [25]. To prepare oxidized LDL (Ox-LDL), LDL was dialysed against PBS to remove EDTA. LDL (0.1 mg/ml) was then incubated with a 5 μ mol/l solution of CuSO₄ at 37°C for 24 h, followed by the addition of 1 mmol/l EDTA and cooling.

Protein labelling with ¹¹¹In and ¹²⁵I BSA, GA-BSA, and MG-BSA were labelled with ¹¹¹In using diethylenetriaminepentaacetic acid (DTPA) as the bifunctional chelating agent as described previously [26]. DTPA was attached to BSA by dissolving the protein (5 mg) in 1.0 ml of 0.1 mol/l HEPES buffer (pH 7.0), and then adding 50 μ g of DTPA anhydride in 10 μ l of DMSO. After stirring for 1 h at room temperature, unreacted DTPA was removed by placing the solution on a Sephadex G-25 column (1 \times 40 cm) followed by elution with 0.1 mol/l sodium acetate buffer (pH 6.0). Fractions containing DTPA-BSA were combined based on the absorption at 280 nm and concentrated by an ultrafiltration apparatus from Advantec (Dublin, CA, USA). Twenty microlitres of ¹¹¹InCl₃ solution, 60 μ l of DTPA-BSA, and 20 μ l of 1 mol/l sodium acetate buffer (pH 6.0) were added. After incubation for 30 min at room temperature, unreacted ¹¹¹InCl₃ was removed by adding the solution to a PD-10 column followed by elution with 0.1 mol/l sodium acetate buffer (pH 6.0). The ¹¹¹In-enriched fractions were selected on the basis of their radioactivity and concentrated by ultrafiltration. Radioactivity was determined with a well counter. The specific activities of ¹¹¹In-BSA, ¹¹¹In-GA-BSA, and ¹¹¹In-MG-BSA were 12 \times 10⁶, 11 \times 10⁶ and 11 \times 10⁶ cpm/mg protein, respectively.

GA-BSA and MG-BSA were labelled with ¹²⁵I by Iodo-Gen (Pierce). A solution containing 10 μ l of Na¹²⁵I solution and 0.5 mg of BSA in 0.2 ml of 0.1 mol/l sodium phosphate buffer (pH 7.4) in a Iodo-Gen-adhered test tube was incubated for 30 min at room

temperature. Unreacted Na I was removed by adding the solution to a PD-10 column followed by elution with PBS. The I-labelled fractions were combined on the basis of their radioactivity, as determined with a well counter. The specific activities of GA-BSA and MG-BSA were 800 and 900 cpm/ng protein, respectively.

Clearance experiments Prior to intravenous administration, trace amounts of ^{111}In -BSA, ^{111}In -GA-BSA, or ^{111}In -MG-BSA were diluted with saline, and the protein concentration was adjusted to 0.1 mg/ml. Each radiolabeled protein (0.1 mg/kg, 10 kcpm) was injected as a bolus into the tail vein of male ddY mice at 7 weeks of age after being anaesthetised with diethylether [27]. After 1, 3, 5, 10, 15, or 20 min, the animals were killed, and the kidney and the liver were excised, followed by a determination of their radioactivities for kidney and liver clearance. To determine the organ distribution of each ^{111}In -labelled protein, the animals were similarly killed at 20 min after injection, and organs such as kidney, liver, pancreas, spleen, lung, heart, and brain were excised to determine their radioactivity. Care and treatment of the animals was in compliance with the "Principles of Laboratory Animal Care" (NIH publication no. 85-23, revised 1985). The protocol was approved by the University of Kumamoto institutional review board for animal procedures.

Data analyses In this study, the radioactivity of liver and kidney samples was used to calculate the apparent uptake clearances of BSA, GA-BSA, and MG-BSA. The radioactivity of all samples and that of the plasma was normalised to the percentage of dose or percentage of dose per millilitre, respectively. Plasma concentrations were analysed by a biexponential function using the non-linear least-squares computer program MULTI [28]. The two-compartment model was chosen according to the Akaike information criterion. Total body clearance of radioactivity (CL_{total}) was calculated by:

$$\text{CL}_{\text{total}} = \frac{D}{\text{AUC}}$$

where D is the dose of radioactivity administered, and AUC is the area under the plasma concentration–time curve extrapolated to infinity.

Assuming zero or negligible leakage of radioactivity from organs, the apparent organ uptake clearance (CL_{organ}) may be expressed as:

$$\text{CL}_{\text{organ}} = \frac{X_{t_i}}{\text{AUC}_{t_0 - t_i}}$$

where X_{t_i} is the amount of radioactivity in the organ of interest at the end of the experiment, and $\text{AUC}_{t_0 - t_i}$ is the area under the curve for the time interval from t_0 = administration of the compound, to t_i = end of the experiment.

Preparation of biotinylated antibody against GA-BSA The monoclonal anti-GA-BSA antibody was prepared and purified by protein G-immobilised Sepharose gel chromatography to IgG1, as described previously [5]. This monoclonal antibody was shown to be specific for the glycolaldehyde-derived pyridine (GA-pyridine) structure [5] and is referred to as the anti-GA-pyridine antibody in the present study [5]. The anti-GA-pyridine antibody (0.5 mg) was biotinylated by reaction with 50 μ g of BNHS for 1 h at room temperature in 0.1 mol/l carbonate buffer (pH 8.4) and dialysed against PBS to remove unreacted BNHS. The immunoreactivity of the biotinylated antibody for GA-BSA was indistinguishable from the unlabelled anti-GA-pyridine antibody as determined by ELISA.

Immunohistochemistry GA-BSA (5 mg/kg) was injected as a bolus into the tail vein of male C57BL/6 mice at 7 weeks of age after being anaesthetised with diethylether. After 5 min, the animals were killed, and the kidneys removed, fixed with a 2% periodate/lysine/paraformaldehyde fixative at 4°C for 5 h and washed with PBS containing a graded series of sucrose (10, 15 and 20%). After immersion in PBS containing 20% sucrose to inhibit ice crystal formation, the tissues were embedded in OCT compound (Sakura Fine Technical, Tokyo, Japan), frozen in liquid nitrogen, and stored at -80°C until used. Sections were cut 5- μ m thick with a cryostat (HM-500 M; Microm, Walldorf, Germany) and mounted on poly-L-lysine-coated slides.

For immunohistochemical analysis, cryostat sections were prepared and examined by the indirect immunoperoxidase method. Briefly, after inhibition of endogenous peroxidase activity by the method of Isobe et al. [29], the sections were incubated with 10 μ g/ml of

biotinylated anti-GA-pyridine antibody, washed with PBS, and reacted with streptavidin/HRP (DAKO). After visualisation with 3,3'-diaminobenzidine (Dojin Chemical, Kumamoto, Japan), the sections were counterstained with haematoxylin (Mutoh Chemical, Tokyo, Japan). For negative controls, the identical procedures were performed, but the antibody and the biotinylated antibody were omitted. Non-immune mouse IgG1 was also used as a negative control, and staining showed no evidence for an immunoreaction. For the immunoabsorption test, 10 μ g/ml of biotinylated anti-GA-pyridine antibody was preincubated with 10 μ g/ml of GA-BSA at 37°C for 1 h and allowed to react with streptavidin/HRP.

Cellular experiments with mesangial cells Isolation of glomerular cores was performed by the method of Mori et al. [30] with a minor modification. Briefly, the kidneys of male ddY mice at 7 weeks of age were removed under anaesthesia with diethylether and cut into slices. Each slice was pressed through a 425- μ m-pore-size sieve. The pass-through was rinsed three times in HBSS and pellets were centrifuged at 3,000 rpm for 10 min. The pellets were then incubated for 30 min at 37°C with 750 U/ml of collagenase in 5 ml of HBSS, followed by washing three times with HBSS for centrifugation and passing through two sieves with pore sizes of 100 and 40 μ m. The glomerular cores remaining on the finest sieve were cultured at 37°C for 2 weeks in RPMI 1640 medium with

20% FCS, 100 U/ml penicillin, 10 μ g/ml streptomycin, and ITS premix in 75-cm² plastic tissue culture flasks in a 5% CO₂ incubator. Mesangial cells obtained from the fifth to eighth passage were plated on 12-well plates at 7.5 × 10⁴ cells/well and cultured for 24 h at 37°C in RPMI 1640 medium with 20% FCS, 100 U/ml penicillin, and 10 μ g/ml streptomycin before each experiment described below. Except for the binding experiments described below, all cellular experiments were performed at 37°C in a humidified atmosphere of 5% CO₂ in air.

Cultured mesangial cells used in the present study formed a uniform cell population based on the following criteria: (1) spindle shape; (2) positive immunohistochemistry for both β -actin (Fig. 1a) and vimentin (Fig. 1b), but negative for cytokeratin (Fig. 1c) and Factor VIII (Fig. 1d); (3) contraction in response to angiotensin II and vasopressin; and (4) induction of TGF- β by serotonin [31].

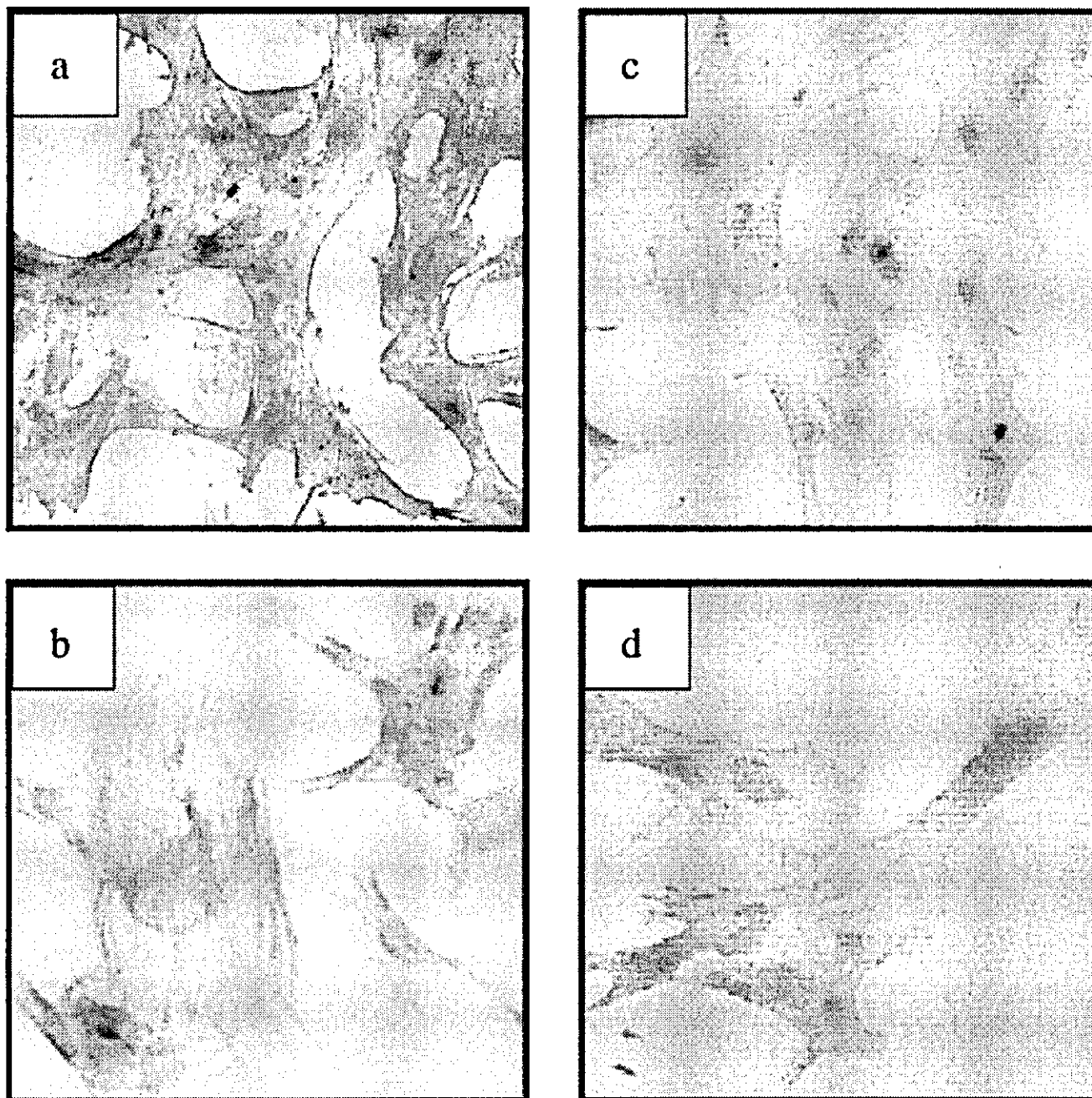


Fig. 1 Immunohistochemical staining for β -actin (a), vimentin (b), cytokeratin (c) and Factor VIII (d) in mouse mesangial cells. Staining of mouse mesangial cells between the fifth and eighth passages was positive for β -actin (a) and vimentin (b), but negative for cytokeratin (c) and Factor VIII (d)

An additional note to the method: although our modified method—sieving of glomerular cores after collagenase treatment—gives a high yield of glomerular cores and subsequent mesangial cells, special attention has to be paid to the possibility that incubation with collagenase could lead to the overdigestion of glomerular cores and a low yield of glomerular core on the finest sieve. To prevent this, the readers are highly recommended to do preliminary experiments to determine the adequate incubation time for collagenase treatment as well as selection of the suitable collagenase batch from commercially available ones.

For binding experiments, confluent mesangial cells were washed twice with 1.0 ml of PBS and incubated for 90 min at 4°C with 1.0 ml of DMEM supplemented with 3% (w/v) BSA containing the indicated concentrations of ^{125}I -GA-BSA or ^{125}I -MG-BSA with or without a 50-fold excess of unlabelled GA-BSA or MG-BSA. After washing three times with ice-cold PBS containing 1% (w/v) BSA and twice further with PBS, the cells were dissolved in 1.0 ml of 0.1 mol/l NaOH, and cell-bound radioactivity and cellular proteins were determined.

For uptake and degradation experiments, confluent cells were washed twice with PBS and incubated at 37°C with 1.0 ml of DMEM supplemented with 3% (w/v) BSA containing the indicated concentrations of ^{125}I -GA-BSA or ^{125}I -MG-BSA with or without a 50-fold excess of unlabelled GA-BSA or MG-BSA. After incubation for the indicated time intervals, culture medium (0.75 ml) was taken from each well and mixed with 0.3 ml of 40% trichloroacetic acid on a vortex mixer. To this solution was added 0.2 ml of 0.7 mol/l AgNO₃, followed by centrifugation. The resulting supernatant was used to determine trichloroacetic acid-soluble radioactivity, which

3
was taken as an index of cellular degradation, since AGE proteins are endocytosed by the cells and delivered to lysosomes where they are degraded and excreted into the culture medium in a trichloroacetic acid-soluble form. The remaining cells in each well were washed three times with 1.0 ml of PBS containing 1% (w/v) BSA and twice more with PBS. The cells were lysed at 37°C for 30 min with 1.0 ml of 0.1 mol/l NaOH. One portion was used to determine the radioactivity of the cell-associated ligand and the other was used to determine cellular proteins using the bicinchoninic acid protein assay reagent (Pierce) [32].

For inhibition assays, mesangial cells were incubated at 4°C for 90 min with 2.5 $\mu\text{g/ml}$ of ^{125}I -GA-BSA or ^{125}I -MG-BSA in the absence (control) or presence of 40-fold (100 $\mu\text{g/ml}$) of unlabelled ligands such as GA-BSA, MG-BSA, Ox-LDL, Ac-LDL, and LDL. The extents of cell-bound ^{125}I -GA-BSA and ^{125}I -MG-BSA were determined as described above.

Statistical analysis Data are expressed as mean \pm SD. Differences between groups were evaluated by paired Student's *t*-test. A *p* value less than 5% denoted a statistically significant difference.

Results

Plasma clearance of GA-BSA and MG-BSA Figure 2 shows the plasma clearance in mice that had been intravenously injected with ^{111}In -BSA, ^{111}In -GA-BSA, and ^{111}In -MG-BSA; the clearance rate of ^{111}In -BSA was very slow, whereas the radioactivity of ^{111}In -GA-BSA or ^{111}In -MG-BSA was rapidly cleared from the circulation, with about 80% of the injected ^{111}In -GA-BSA or ^{111}In -MG-BSA being eliminated within 5 min after intravenous administration. Figure 3 shows tissue distribution of ^{111}In -BSA, ^{111}In -GA-BSA, and ^{111}In -MG-BSA. At 20 min after the injection of ^{111}In -GA-BSA, 38% of the total injected radioactivity accumulated in the liver, and its renal accumulation corresponded to 21% (Fig. 3b). A similar pattern was obtained for ^{111}In -MG-BSA, with 32% for hepatic accumulation and 19% for renal accumulation (Fig. 3c). Accumulation by other organs such as pancreas, spleen, lung, heart, and brain was negligibly low, and the pattern was indistinguishable from that of BSA (Fig. 3a).

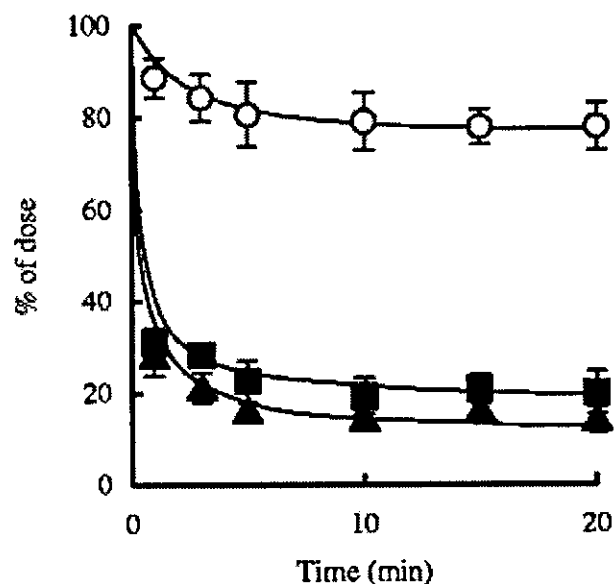


Fig. 2 Plasma clearance of ^{111}In -BSA, ^{111}In -GA-BSA, and ^{111}In -MG-BSA after intravenous administration to mice; ^{111}In -BSA (open circles), ^{111}In -GA-BSA (closed triangles), and ^{111}In -MG-BSA (closed squares) were injected as a bolus through the tail vein of mice, and the relative radioactivities are plotted against time after injection. Each data point represents the mean \pm SD for three mice

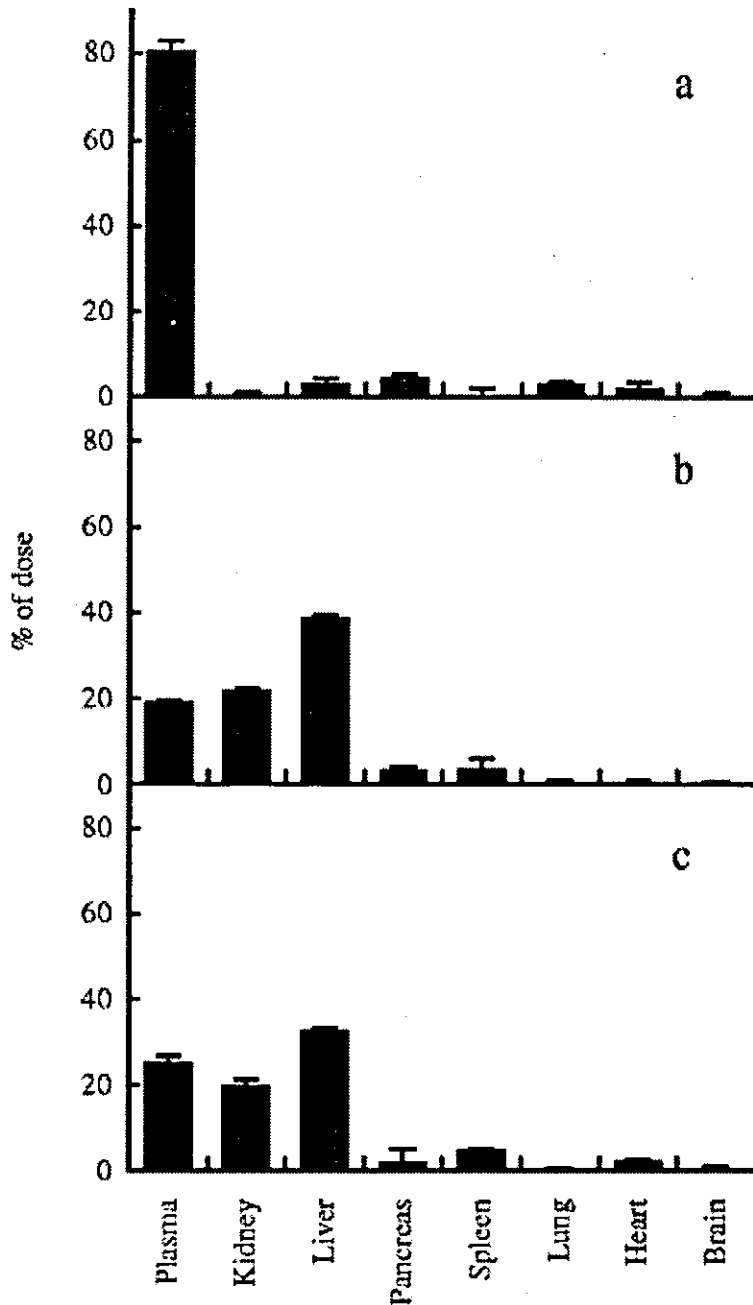


Fig. 3 Anatomical distribution of intravenously injected ^{111}In -BSA (a), ^{111}In -GA-BSA (b), and ^{111}In -MG-BSA (c). The mice used for plasma clearance studies (Fig. 2) were analysed for anatomical distribution of radioactivity 20 min after the injection. Approximately 90% of the injected dose was recovered in the tissues listed in all experiments. Results are means \pm SD for three separate experiments

The clearance rates for liver and kidney were also calculated using the nonlinear least-squares computer program MULTI (Table 1). These CL_{liver} and $\text{CL}_{\text{kidney}}$ values for GA-BSA and MG-BSA were significantly larger than those for BSA, suggesting the presence of a selective uptake system for GA-BSA and MG-BSA in both the liver and kidney.

Table 1 Uptake of ^{111}In -BSA, ^{111}In -GA-BSA and ^{111}In -MG-BSA by mice liver and kidney

	Clearance ($\mu\text{l/h}$)		
	CL_{total}	CL_{liver}	$\text{CL}_{\text{kidney}}$
BSA	57.2 ± 18.1	6.3 ± 3.2	6.9 ± 2.7
GA-BSA	$16,573.8 \pm 1,173.5$	$9,123.5 \pm 603.2$	$3,767.2 \pm 481.6$
MG-BSA	$11,615.6 \pm 869.2$	$5,546.3 \pm 251.3$	$2,505.3 \pm 338.2$

Values are means \pm SD of three sets of experiments

Immunohistochemical distribution in kidney of intravenously injected GA-BSA To determine the cells responsible for renal clearance of AGE proteins from the circulation, the distribution of intravenously administered GA-BSA in the kidney was examined immunohistochemically using the biotinylated anti-GA-pyridine antibody as described in "Materials and methods". At 5 min after an intravenous injection of GA-BSA, positive immunoreactivities were found in the glomerular area with mesangial cells and endothelial cells being the main cellular components (Fig. 4a). These positive immunoreactions in the glomerulus were completely inhibited when the biotinylated antibody was pretreated with 10 μ g/ml of GA-BSA (Fig. 4c). Furthermore, no positive immunoreactions were found in the renal glomerulus when the mice were subjected to an intravenous injection of BSA (Fig. 4d). It seems likely from these immunohistochemical data that mesangial cells, at least, are responsible for the renal clearance of intravenously administered GA-BSA.

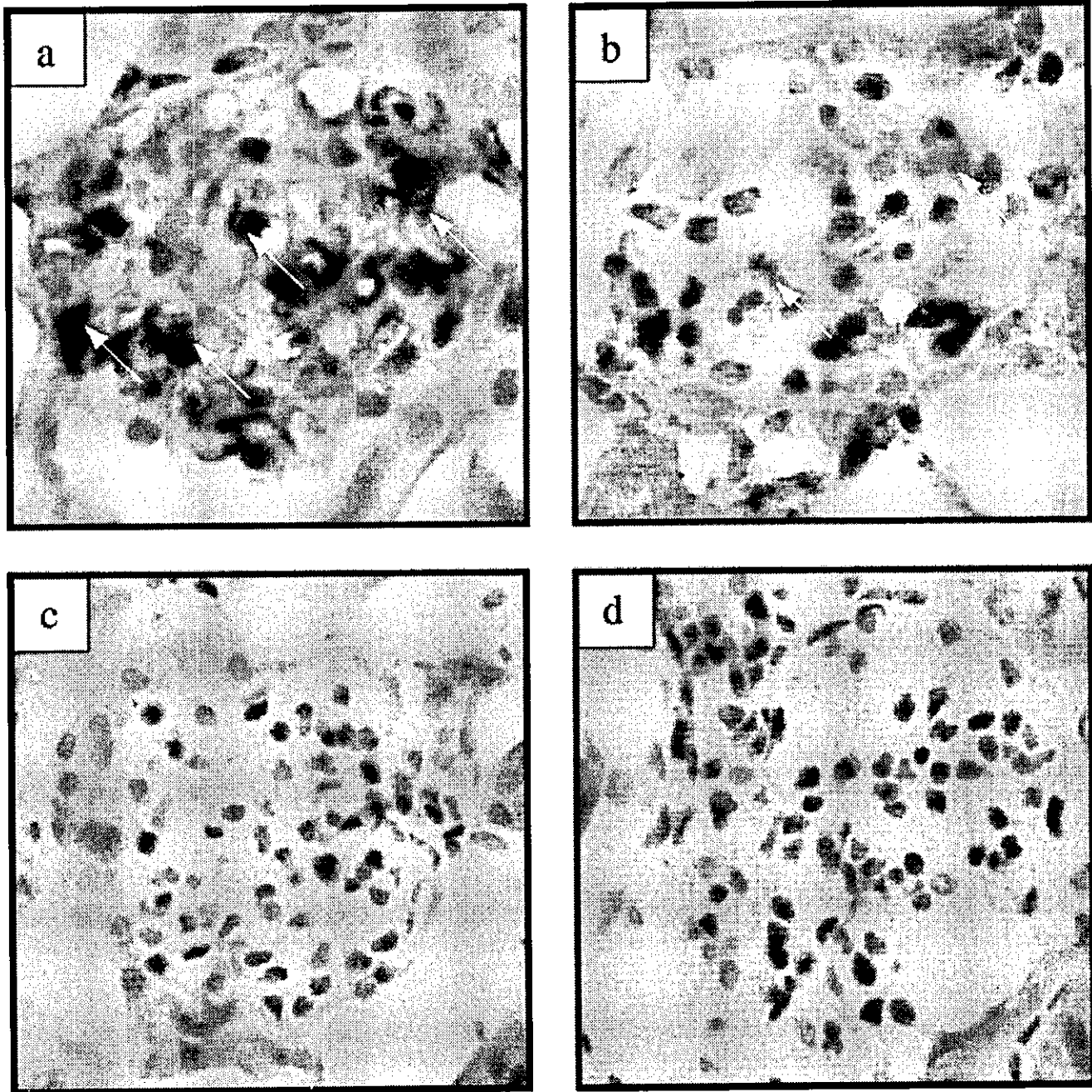


Fig. 4 Immunohistochemical localisation in kidney of GA-BSA after its intravenous administration to mice. The kidney was removed 5 min after an injection of GA-BSA or BSA in the form of a bolus through the tail veins of mice. **a** Anti-GA-pyridine antibody-positive products were observed in mesangial cells and endothelial cells in glomerulus obtained from mice that had been administered GA-BSA (arrows). **b** Positive reactions for anti-GA-pyridine antibody in glomerular areas observed in (a) were significantly weakened in SR-A knock-out mice. **c** Such positive reactions disappeared after preincubation of the antibody with 10 μ g/ml of GA-BSA. **d** No immunoreactivity of anti-GA-pyridine antibody was detected in the glomerulus obtained from mice administered BSA

GA-BSA and MG-BSA undergo receptor-mediated endocytosis by mesangial cells To determine the mechanism for the selective accumulation of intravenously injected GA-BSA and MG-BSA in the mesangium, we examined the cellular interaction of GA-BSA and MG-BSA using isolated mesangial cells. The total binding of ^{125}I -GA-BSA to these cells at 4°C was inhibited by $>80\%$ by the presence of an excess amount of unlabelled GA-BSA (Fig. 5a). The specific binding, which was obtained by subtracting non-specific binding from the total binding, showed a saturation curve for which Scatchard analysis revealed a binding site with an apparent K_d of $6.93 \mu\text{g/ml}$ and a maximal binding of 94.11 ng/mg of cell protein (Fig. 5a, inset). The specific binding of MG-BSA to mesangial cells was also saturable (Fig. 5b), the Scatchard analysis of which gave a binding site with an apparent K_d of $6.80 \mu\text{g/ml}$ and a maximal surface binding of 27.69 ng/mg of cell protein (Fig. 5b, inset). These results indicate that mesangial cells possess a high-affinity binding site for GA-BSA and MG-BSA.

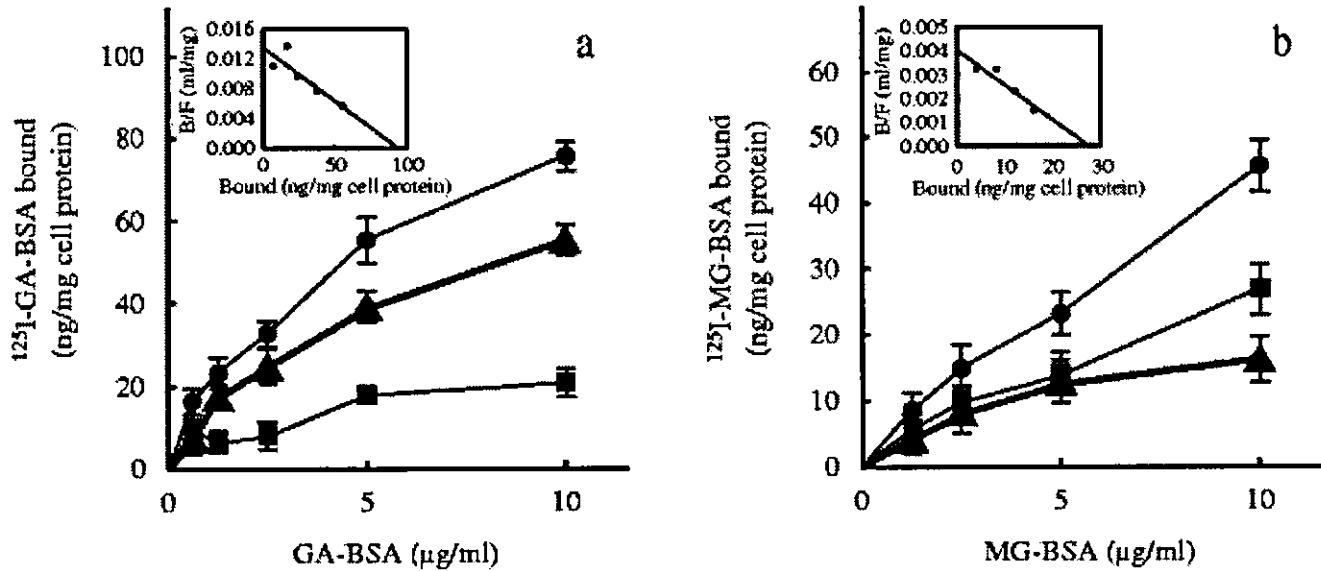


Fig. 5 Binding of ^{125}I -GA-BSA (a) and ^{125}I -MG-BSA (b) to mouse mesangial cells. Mesangial cells were incubated at 4°C for 90 min with the indicated concentrations of ^{125}I -GA-BSA (a) or ^{125}I -MG-BSA (b) in the presence (closed squares) or absence (closed circles) of 50-fold unlabelled ligands. Closed triangles indicate the specific binding of each ligand. Inset Scatchard analysis based on specific binding results for GA-BSA (a) and MG-BSA (b) to mesangial cells. Results are the means \pm SD of three separate experiments

To determine the post-binding outcome of GA-BSA and MG-BSA, these mesangial cells were incubated with ^{125}I -GA-BSA and ^{125}I -MG-BSA at 37°C . The amount of cell-associated ^{125}I -GA-BSA increased with time (Fig. 6a) followed by a parallel increase in the amount of ^{125}I -GA-BSA degraded by these cells (Fig. 6b). In a similar fashion, the amount of ^{125}I -MG-BSA associated with (Fig. 6c) and those degraded by these cells (Fig. 6d) increased with time. Based on these experiments, it appears likely that mesangial cells express receptors that are specific for GA-BSA and MG-BSA, and that ligands that bind to these receptors undergo receptor-mediated endocytosis.

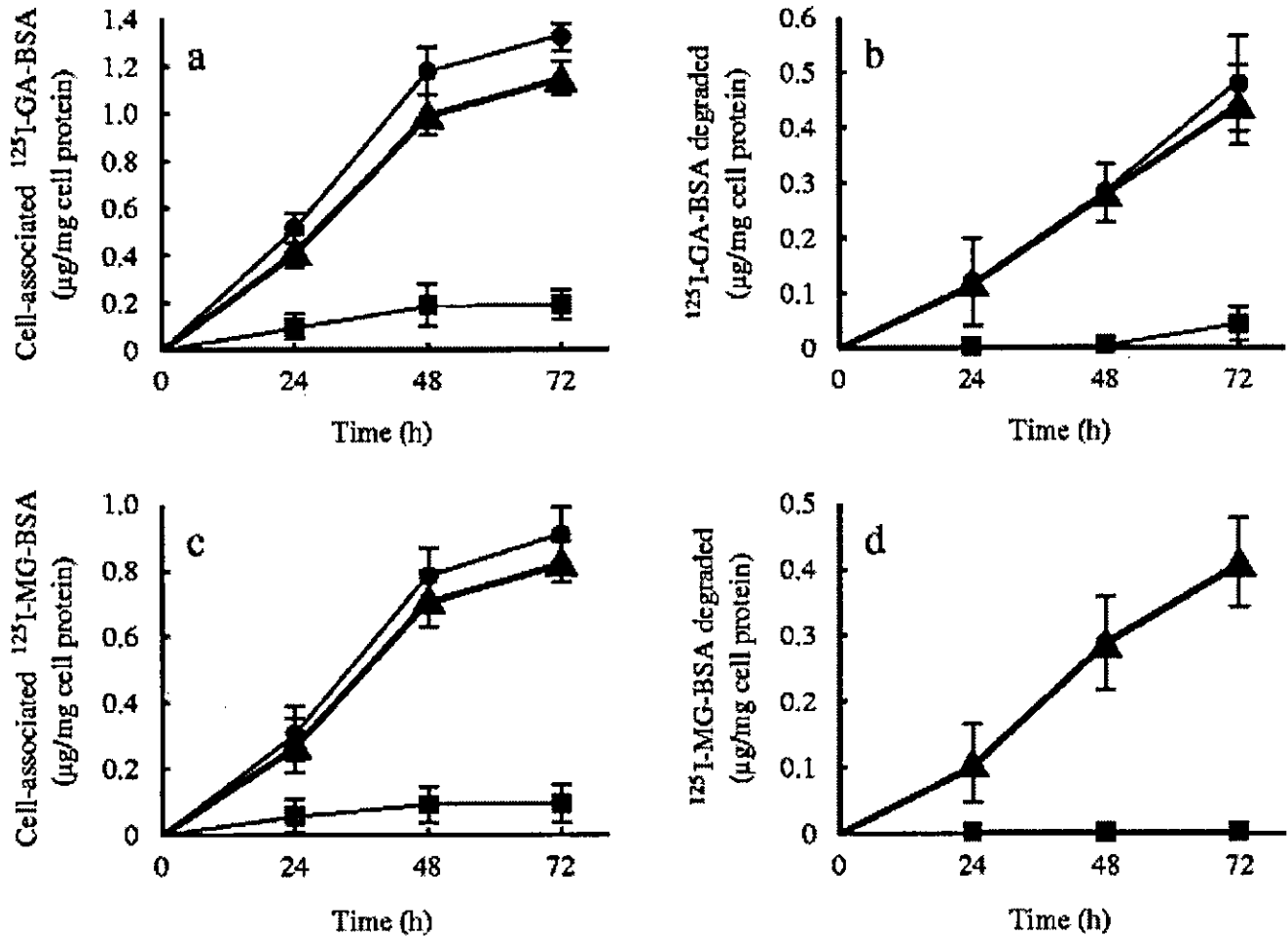


Fig. 6 Time-dependent endocytic uptake (a, c) and degradation (b, d) by mouse mesangial cells of ^{125}I -GA-BSA (a, b) and ^{125}I -MG-BSA (c, d). Mesangial cells were incubated at 37°C for the indicated times with 5×10^{-14} g/ml of ^{125}I -GA-BSA or ^{125}I -MG-BSA in the presence (closed squares) or absence (closed circles) of 50-fold unlabelled ligands. Closed triangles indicate the specific association or degradation of each ligand. The amounts of cell-associated ^{125}I -GA-BSA and ^{125}I -MG-BSA and their degradation were determined as described in Materials and methods. Results are the means \pm SD of three separate experiments

To characterise the receptor for GA-BSA and MG-BSA on mesangial cells, we tested the effects of several ligands for scavenger receptors, such as Ac-LDL and Ox-LDL. The binding of ^{125}I -GA-BSA was effectively inhibited not only by unlabelled GA-BSA but also by MG-BSA, Ac-LDL, and Ox-LDL, whereas LDL showed no significant effect (Fig. 7a). Similarly, the binding of ^{125}I -MG-BSA was effectively inhibited by unlabelled GA-BSA, MG-BSA, Ac-LDL, and Ox-LDL, but not by LDL (Fig. 7b). These results suggest that GA-BSA and MG-BSA are recognised by mesangial cells via a scavenger receptor(s) and undergo receptor-mediated endocytosis.

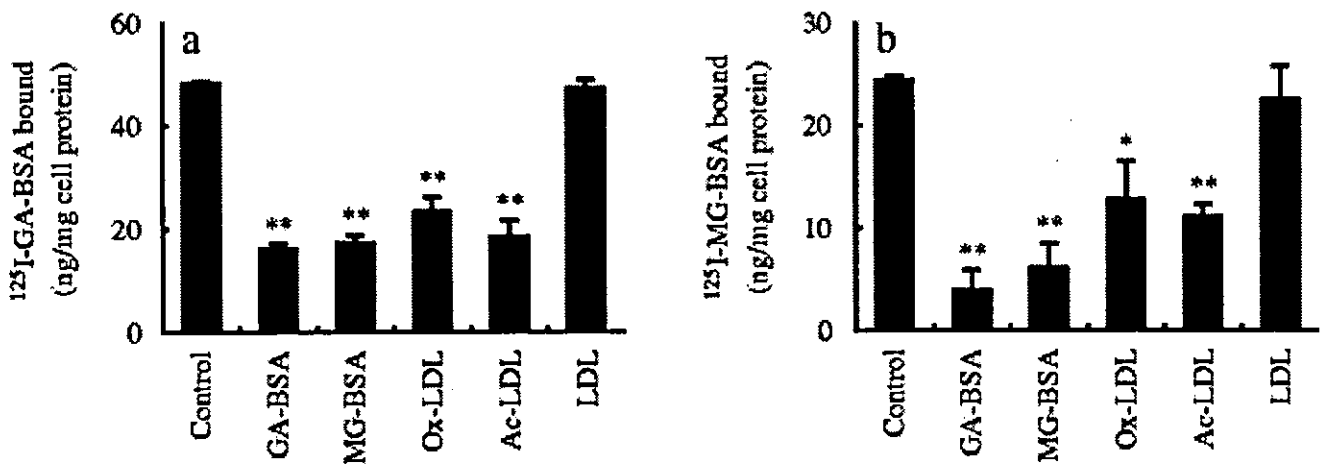


Fig. 7 Effects of several ligands on binding to mouse mesangial cells of ^{125}I -GA-BSA (a) and ^{125}I -MG-BSA (b). Mesangial cells were

incubated at 4°C for 90 min with 2.5 μ g/ml of 125 I-GA-BSA or 125 I-MG-BSA in the absence (control) or the 40-fold presence of unlabelled ligands such as GA-BSA, MG-BSA, Ox-LDL, Ac-LDL, and LDL. The extent of cellular binding of 125 I-GA-BSA and 125 I-MG-BSA was determined as described in *Materials and methods*. Results are the means \pm SD of three separate experiments; * p <0.05, ** p <0.01, compared with the control

Endocytic uptake of GA-BSA by mesangial cells from SR-A knock-out mice Among the scavenger receptors, SR-A [17], CD36 [18], SR-BI [19], and LOX-1 [20] have been identified as the AGE receptors. In this study we determined the extent of contribution of SR-A to the endocytic degradation of GA-BSA by mesangial cells. The specific binding of 125 I-GA-BSA to mesangial cells from SR-A knock-out mice was reduced by 37%, compared with that of wild-type mesangial cells. The extent of subsequent endocytic degradation of 125 I-GA-BSA by mesangial cells from SR-A knock-out mice was reduced by more than 80%, compared with those of wild-type cells (Fig. 8). These results suggest that SR-A probably plays a major role in the endocytic degradation of GA-BSA by mesangial cells.

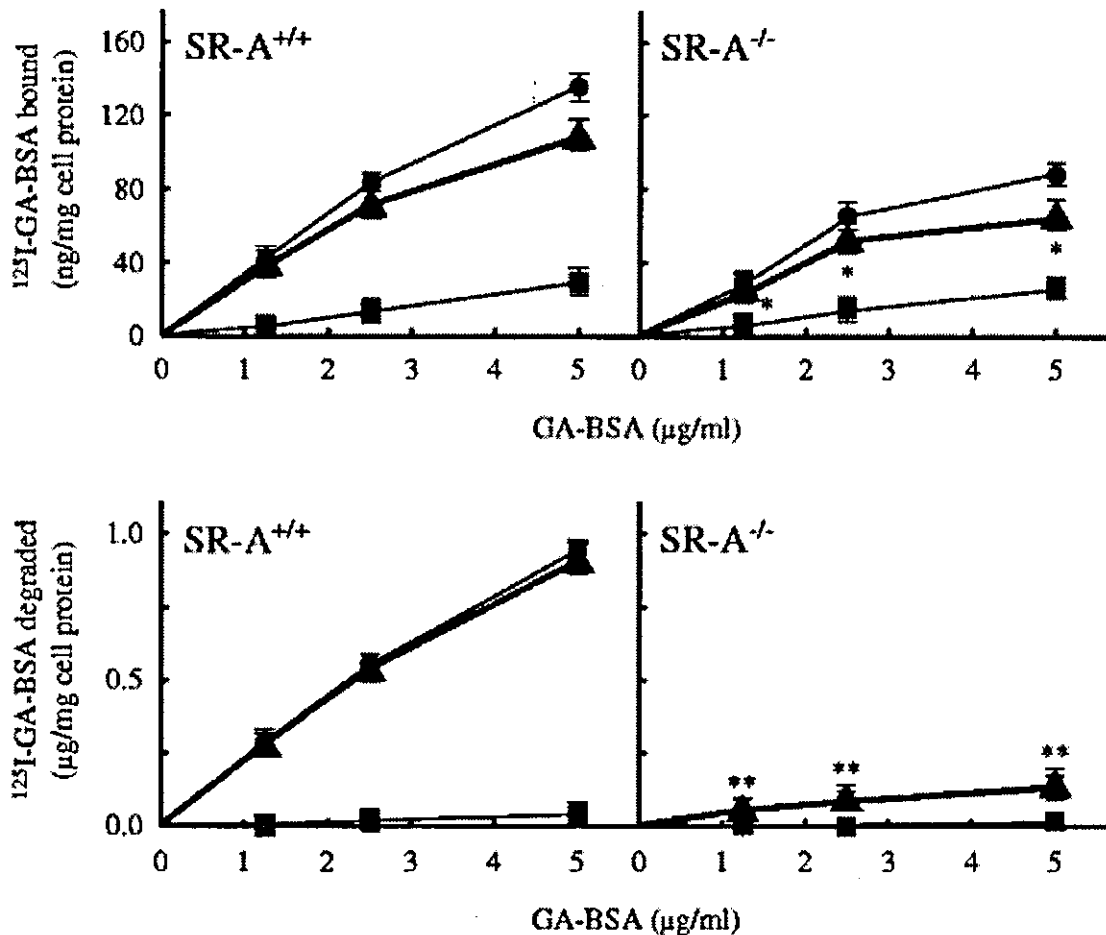


Fig. 8 Binding to, and endocytic degradation by, mesangial cells from SR-A knock-out mice of 125 I-GA-BSA. Mesangial cells obtained from SR-A knock-out mice (right; SR-A^{-/-}) and their littermates (left; SR-A^{+/+}) were incubated at 4°C for 90 min (upper panels) or 37°C for 72 h (lower panels) with the indicated concentrations of 125 I-GA-BSA in the presence (closed squares) or absence (closed circles) of 50-fold unlabelled ligands. Closed triangles indicate the specific binding or degradation of 125 I-GA-BSA. Results are the means \pm SD of three separate experiments; * p <0.05, ** p <0.01, compared with the corresponding concentration for the specific binding and endocytic degradation of SR-A^{+/+}

To elucidate whether the renal uptake of circulating AGE proteins is mediated through the SR-A pathway in vivo, immunohistochemical experiments with kidneys after the injection of GA-BSA to SR-A knock-out mice were undertaken. Positive reactions were observed in mesangial cells and endothelial cells in wild-type mice (Fig. 4a), but the same reactions in SR-A knock-out mice were less (Fig. 4b), suggesting the glomerular accumulation of GA-BSA from the circulation via SR-A in vivo.

Discussion

The findings herein show that GA-BSA and MG-BSA leave the circulation rapidly and accumulate in the liver and kidney (Fig. 3).

Schmidt et al. [33] prepared AGE-BSA by incubating BSA with 250 mmol/l glucose-6-phosphate at 37°C for 4 weeks and reported that its plasma clearance in mice was rapid with 70% of the injected dose being removed from the circulation within 5 min. The amount of organ distribution at 10 min after intravenous injection was 43% for the liver, 17% for the lung, and 7% for the kidney, suggesting that the liver was the main organ for plasma clearance, but the removal by lungs and kidneys was not negligible. Vlassara et al. [34] prepared AGE rat serum albumin (RSA) by incubating RSA with 50 mmol/l glucose-6-phosphate at 37°C for 6 weeks, and its daily intravenous injection for 5 months (25 mg/kg per day) resulted in the induction of glomerular hypertrophy under which renal AGE accumulation was 1.5-fold higher than the controls, suggesting that intravenously administered AGE proteins could be trapped by the kidney *in vivo*. The results of the present study consistently showed that intravenously injected ¹¹¹In-labelled GA-BSA or MG-BSA in mice led to a significant renal accumulation of these ligands: 21% for GA-BSA and 19% for MG-BSA at 20 min after injection. However, data reported by Smedsrød et al. [35] are somewhat different: AGE-BSA prepared by incubating BSA with 1.7 mol/l of glucose for 40 weeks at 37°C was labelled with ¹²⁵I and its hepatic and renal accumulation determined after intravenous injection; the hepatic accumulation was dominant (94%) whereas the renal accumulation of ligands was very low (2.4% of the total injected radioactivity) at 60 min after an intravenous administration in the rat. It is not clear why the extent of renal accumulation after an intravenous injection of these AGE ligands differs from one experiment to another. It could reflect a difference in conditions used in preparing AGE proteins. Alternatively, the difference could be due to the method used for protein labelling. The present study used ¹¹¹In-labelled ligands whereas previous studies had used ¹²⁵I-labelled ligands. Proteins labelled with ¹¹¹In are known to have several advantages over those labelled with ¹²⁵I. The exchange of ¹¹¹In from ¹¹¹In-labelled proteins to other proteins in the lysosome results in a better target retention of radioactivity, whereas an ¹²⁵I-labelled protein can be degraded in lysosomes and released outside the cells, and the resulting amount of ¹²⁵I radioactivity accumulated in tissues could be underestimated [27].

For the accumulation of intravenously injected GA-BSA in the kidney, an immunoreaction for the anti-GA-pyridine antibody was found in the mesangial and endothelial cell areas (Fig. 4a). In this context, previous immunohistochemical studies using anti-AGE antibodies (mainly anti-CML antibodies) revealed the accumulation of AGE proteins in the mesangial lesions in diabetic nephropathy [8, 9]. In addition, an immunohistochemical study demonstrated the presence of SR-A on mesangial cell membranes in renal biopsy specimens from patients with glomerular diseases [21]. RT-PCR analyses revealed the expression of AGE receptors including OST-48, 80 K-H, and galectin-3 complex in mesangial cells that had been isolated from both normal and diabetic mice, and binding experiments using AGE-BSA with these cells revealed a specific binding with an apparent Kd of 160–300 nmol/l [22]. Binding experiments using AGE-BSA with membrane fractions isolated from rat and human mesangial cells revealed a saturable binding with a Kd of 500 nmol/l [36]. Finally, from the present study, it is clear that mouse mesangial cells are able to efficiently endocytose and degrade GA-BSA and MG-BSA (Figs. 5 and 6). Collectively, these data indicate that it is likely that mesangial cells are responsible for the renal uptake of AGE proteins from the circulation.

The present result shows that GA-BSA and MG-BSA bind to mouse mesangial cells, and that this binding is effectively inhibited by Ox-LDL and Ac-LDL as well as by MG-BSA, but not by LDL (Fig. 7). This indicates that the ligand specificity of the receptor involved is similar to that of scavenger receptors rather than that of RAGE, OST-48, 80 K-H, and galectin-3 complex. Consistent with this observation, a previous study showed that ¹²⁵I-Ox-LDL was degraded by rat mesangial cells, and that this process was effectively inhibited by unlabelled Ac-LDL, suggesting the involvement of scavenger receptor(s) [37]. Four scavenger receptors have been identified as AGE receptors: SR-A [17], CD36 [18], SR-BI [19], and LOX-1 [20]. Since a previous immunohistochemical study using an anti-SR-A antibody showed the presence of SR-A in human mesangial cells [21], and we also confirmed the expression of SR-A mRNA in mouse mesangial cells (data not shown), the contribution of SR-A to the endocytic uptake of these AGE proteins by mesangial cells was assessed in the present study. Our experiments with mesangial cells from SR-A knock-out mice indicate that SR-A contributes ~40% to the binding and ~80% to the subsequent degradation of AGE-modified proteins. The difference in contribution of SR-A to binding and degradation is not clear at present, but might be explained by (1) the expression of other AGE receptors such as RAGE, OST-48, 80 K-H, and galectin-3 complex in mesangial cells [22, 23] and (2) the fact that these receptors do not belong to the endocytosis-coupled receptor (ligand binding to these receptor does not follow the subsequent endocytic uptake, in sharp contrast to SR-A).

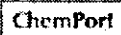





A recent study using SR-A knock-out mice has clarified the crucial role of SR-A in the pathogenesis of diabetic nephropathy; diabetic wild-type mice showed typical signs of diabetic nephropathy such as an increase in urinary albumin excretion, glomerular hypertrophy, an increase in mesangial matrix and fibrosis in interstitial tissues, whereas these pathologies were effectively ameliorated in diabetic SR-A knock-out mice (Shikata et al., personal communication).








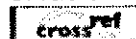
In summary, the earliest morphological abnormalities in diabetic nephropathy are the thickening of the glomerular basement membrane and the expansion of mesangial lesions due to the accumulation of extracellular matrix [38]. The interaction of AGE-modified proteins with mesangial cells led to an increased production of collagen, fibronectin, laminin, and proteoglycan [12, 13]. Therefore, the present study provides new evidence indicating that circulating AGE-modified proteins are cleared from the kidney by SR-A-mediated endocytic uptake by mesangial cells, suggesting that AGE proteins delivered by this pathway might play some role in the pathogenesis of diabetic nephropathy.






Acknowledgements This work was supported, in part, by grants-in-aid for scientific research from the Ministry of Education, Science, Sports and Culture of Japan (11694298; 11794016).

References

1. Maillard LC (1912) Action des acides amines sur les sucres: formation des melanoidines par voie methodique. *C R Acad Sci (Paris)* 154:66–68
2. Horiuchi S, Higashi T, Ikeda K et al (1996) Advanced glycation end products and their recognition by

- macrophage and macrophage-derived cells. *Diabetes* 45:73—76
3. Nagai R, Matsumoto K, Ling X, Suzuki H, Araki T, Horiuchi S (2000) Glycolaldehyde, a reactive intermediate for advanced glycation end products, plays an important role in the generation of an active ligand for the macrophage scavenger receptor. *Diabetes* 49:1714—1723
-  
4. Wells-Knecht KJ, Zyzak DV, Litchfield JE, Thorpe SR, Baynes JW (1995) Mechanism of autoxidative glycosylation: identification of glyoxal and arabinose as intermediates in the autoxidative modification of proteins by glucose. *Biochemistry* 34:3702—3709
5. Nagai R, Hayashi CM, Xia L, Takeya M, Horiuchi S (2002) Identification in human atherosclerotic lesions of GA-pyridine, a novel structure derived from glycolaldehyde-modified proteins. *J Biol Chem* 277:48905—48912
- 
6. Beisswenger PJ, Howell SK, Touchette AD, Lal S, Szwegold BS (1999) Metformin reduces systemic methylglyoxal levels in type 2 diabetes. *Diabetes* 48:198—202
7. Takeuchi M, Makita Z, Bucala R, Suzuki T, Koike T, Kameda Y (2000) Immunological evidence that non-carboxymethyllysine advanced glycation end-products are produced from short chain sugars and dicarbonyl compounds in vivo. *Mol Med* 6:114—125
8. Tanji N, Markowitz GS, Fu C et al (2000) Expression of advanced glycation end products and their cellular receptor RAGE in diabetic nephropathy and nondiabetic renal disease. *J Am Soc Nephrol* 11:1656—1666
9. Sugiyama S, Miyata T, Horie K et al (1996) Advanced glycation end-products in diabetic nephropathy. *Nephrol Dial Transplant* 11:91—94
10. Lal MA, Brismar H, Eklof AC, Aperia A (2002) Role of oxidative stress in advanced glycation end product-induced mesangial cell activation. *Kidney Int* 61:2006—2014
- 
11. Doi T, Vlassara H, Kirstein M, Yamada Y, Striker GE, Striker LJ (1992) Receptor-specific increase in extracellular matrix production in mouse mesangial cells by advanced glycosylation end products is mediated via platelet-derived growth factor. *Proc Natl Acad Sci U S A* 89:2873—2877
12. Pugliese G, Pricci F, Romeo G et al (1997) Upregulation of mesangial growth factor and extracellular matrix synthesis by advanced glycation end products via a receptor-mediated mechanism. *Diabetes* 46:1881—1887
13. Kim YS, Kim BC, Song CY, Hong HK, Moon KC, Lee HS (2001) Advanced glycosylation end products stimulate collagen mRNA synthesis in mesangial cells mediated by protein kinase C and transforming growth factor- β . *J Lab Clin Med* 138:59—68
- 
14. Yamagishi S, Inagaki Y, Okamoto T et al (2002) Advanced glycation end product-induced apoptosis and overexpression of vascular endothelial growth factor and monocyte chemoattractant protein-1 in human-cultured mesangial cells. *J Biol Chem* 277:20309—20315
- 

15. Neepser M, Schmidt AM, Brett J et al (1992) Cloning and expression of a cell surface receptor for advanced glycosylation end products of proteins. *J Biol Chem* 267:14998—15004
16. Li YM, Mitsuhashi T, Wojciechowicz D et al (1996) Molecular identity and cellular distribution of advanced glycation endproduct receptors: relationship of p60 to OST-48 and p90 to 80K-H membrane proteins. *Proc Natl Acad Sci U S A* 93:11047—11052

17. Kodama T, Freeman M, Rohrer L, Zabrecky J, Matsudaira P, Krieger M (1990) Type I macrophage scavenger receptor contains alpha-helical and collagen-like coiled coils. *Nature* 343:531—535

18. Ohgami N, Nagai R, Ikemoto M et al (2001) CD36, a member of the class B scavenger receptor family, as a receptor for advanced glycation end products. *J Biol Chem* 276:3195—3202

19. Ohgami N, Nagai R, Miyazaki A et al (2001) Scavenger receptor class B type I-mediated reverse cholesterol transport is inhibited by advanced glycation end products. *J Biol Chem* 276:13348—13355

20. Jono T, Miyazaki A, Nagai R, Sawamura T, Kitamura T, Horiuchi S (2002) Lectin-like oxidized low density lipoprotein receptor-1 (LOX-1) serves as an endothelial receptor for advanced glycation end products (AGE). *FEBS Lett* 511:170—174

21. Takemura T, Yoshioka K, Aya N et al (1993) Apolipoproteins and lipoprotein receptors in glomeruli in human kidney diseases. *Kidney Int* 43:918—927
22. He CJ, Zheng F, Stitt A, Striker L, Hattori M, Vlassara H (2000) Differential expression of renal AGE-receptor genes in NOD mice: possible role in nonobese diabetic renal disease. *Kidney Int* 58:1931—1940
23. Schmidt AM, Hori O, Brett J, Yan SD, Wautier JL, Stern D (1994) Cellular receptors for advanced glycation end products: Implications for induction of oxidant stress and cellular dysfunction in the pathogenesis of vascular lesions. *Arterioscler Thromb* 14:1521—1528
24. Suzuki H, Kurihara Y, Takeya M et al (1997) A role for macrophage scavenger receptors in atherosclerosis and susceptibility to infection. *Nature* 386:292—296

25. Sakai M, Miyazaki A, Hakamata H et al (1994) Lysophosphatidylcholine plays an essential role in the mitogenic effect of oxidized low density lipoprotein on murine macrophages. *J Biol Chem* 269:31430—31435
26. Hnatowich DJ, Layne WW, Childs RL (1982) The preparation and labeling of DTPA-coupled albumin. *Int J Appl Radiat Isot* 33:327—332

27. Staud F, Nishikawa M, Morimoto K, Takakura Y, Hashida M (1999) Disposition of radioactivity after injection of liver-targeted proteins labeled with ¹¹¹In or ¹²⁵I: effect of labeling on distribution and excretion of radioactivity in rats. *J Pharm Sci* 88:577—585


28. Yamaoka K, Tanigawara Y, Nakagawa T, Uno T (1981) A pharmacokinetic analysis program (multi) for microcomputer. *J Pharmacobiodyn* 4:879—885
 
29. Isobe Y, Nakane PK, Brown WR (1977) Studies on translocation of immunoglobulins across intestinal epithelium, I: improvements in the peroxidase-labeled antibody method for application to study of human intestinal mucosa. *Acta Histochem Cytochem* 10:161—171
30. Mori T, Bartocci A, Satriano J et al (1990) Mouse mesangial cells produce colony-stimulating factor-1 (CSF-1) and express the CSF-1 receptor. *J Immunol* 144:4697—4702
31. Kasho M, Sakai M, Sasahara T et al (1998) Serotonin enhances the production of type IV collagen by human mesangial cells. *Kidney Int* 54:1083—1092

32. Matsumoto K, Sano H, Nagai R et al (2000) Endocytic uptake of advanced glycation end products by mouse liver sinusoidal endothelial cells is mediated by a scavenger receptor distinct from the macrophage scavenger receptor class A. *Biochem J* 352:233—240

33. Schmidt AM, Hasu M, Popov D et al (1994) Receptor for advanced glycation end products (AGEs) has a central role in vessel wall interactions and gene activation in response to circulating AGE proteins. *Proc Natl Acad Sci U S A* 91:8807—8811
34. Vlassara H, Striker LJ, Teichberg S, Fuh H, Li YM, Steffes M (1994) Advanced glycation end products induce glomerular sclerosis and albuminuria in normal rats. *Proc Natl Acad Sci U S A* 91:11704—11708
35. Smedsrød B, Melkko J, Araki N, Sano H, Horiuchi S (1997) Advanced glycation end products are eliminated by scavenger-receptor-mediated endocytosis in hepatic sinusoidal Kupffer and endothelial cells. *Biochem J* 322:567—573
36. Skolnik EY, Yang Z, Makita Z, Radoff S, Kirstein M, Vlassara H (1991) Human and rat mesangial cell receptors for glucose-modified proteins: potential role in kidney tissue remodelling and diabetic nephropathy. *J Exp Med* 174:931—939

37. Jenkins AJ, Velarde V, Klein RL et al (2000) Native and modified LDL activate extracellular signal-regulated kinases in mesangial cells. *Diabetes* 49:2160—2169
38. Adler S (1994) Structure—function relationships associated with extracellular matrix alterations in diabetic glomerulopathy. *J Am Soc Nephrol* 5:1165—1172

Platelet glycoprotein Ib alpha polymorphisms affect the interaction with von Willebrand factor under flow conditions

Yumiko Matsubara,¹ Mitsuru Murata,¹
Tomohiro Hayashi,² Keiji Suzuki,³
Yosuke Okamura,⁴ Makoto Handa,⁵
Hiroaki Ishihara,⁶ Toshiro Shibano⁶
and Yasuo Ikeda¹

¹Department of Medicine, Keio University, Tokyo,

²Department of Medicine, Tohoku Central Hospital, Yamagata, ³Department of Hematology and Oncology, Iwate Medical University, Iwate, ⁴Advanced Research Institute for Science and Engineering, Waseda University, Tokyo, ⁵Blood Center, Keio University, Tokyo, and ⁶New Product Research Laboratories II, Daiichi Pharmaceutical Co. Ltd, Tokyo, Japan

Received 22 October 2004; accepted for publication 29 November 2004

Correspondence: Mitsuru Murata, Department of Medicine, School of Medicine, Keio University, 35 Shinanomachi, Shinjuku-ku, Tokyo 160-8582, Japan.
E-mail: murata@sc.itc.keio.ac.jp

Summary

Interaction of platelet glycoprotein (GP) Ib α with von Willebrand factor (VWF) is essential for thrombus formation, particularly under high shear conditions. Previous case-control studies indicated that two GPIb α polymorphisms, ¹⁴⁵Thr/Met and/or variable number (1–4) tandem repeats of 13 amino-acid sequences, are associated with arterial thrombosis. The ¹⁴⁵Met-allele and the 3R- or 4R-allele is associated with increased risk. However, there is little clear experimental data to support this association. To elucidate the functional effects of these polymorphisms, we prepared recombinant GPIb α fragments and tested them *in vitro*. The dissociation constants of ristocetin-induced ¹²⁵I-labelled VWF binding to two forms of soluble recombinant GPIb α [¹His-³⁰²Ala, either ¹⁴⁵Thr (145T) or ¹⁴⁵Met (145M)] were not different. Four types of Chinese hamster ovary cells expressing full-length GPIb α β /IX, 145T with one repeat (T1R), 145M with one repeat (M1R), 145T with four repeats (T4R), and 145M with four repeats (M4R), were prepared, and cell interactions with immobilized-VWF were examined under various shear conditions. The cell rolling velocity of M4R under a shear condition of 114/s was significantly slower than that of T1R. Intermediate values were obtained with M1R and T4R. The results suggest that M4R interacts more strongly with VWF under flow conditions.

Keywords: polymorphisms, mutagenesis, platelets, glycoprotein Ib alpha, von Willebrand factor.

Glycoprotein (GP) Ib-IX-V complex is a platelet membrane receptor for von Willebrand factor (VWF) (Lopez, 1994; Clemetson, 1997; Ware, 1998; Andrews *et al*, 2003). This receptor consists of four subunits, GP Ib α , Ib β , IX, and V. The largest subunit of the complex, GPIb α , has a VWF-binding site within the N-terminal 45-kDa extracytoplasmic domain of approximately 300 amino acids (Titani *et al*, 1987; Huizinga *et al*, 2002; Uff *et al*, 2002). Interaction of GPIb α with VWF mediates high shear-stress-dependent platelet activation, which is a critical step for thrombus formation (Ikeda *et al*, 1997; Dopheide *et al*, 2001; Ruggeri, 2003). The VWF/GPIb α interaction is not observed under static conditions *in vitro*, but only under shear conditions. Assessment under static conditions requires the presence of non-physiologic inducers, such as ristocetin or botrocetin.

In previous case-control studies, two genetic polymorphisms within the coding region of GPIb α were reportedly

associated with arterial thrombosis, such as coronary artery disease and stroke (Hato *et al*, 1997; Murata *et al*, 1997; Sonoda *et al*, 2000; Simmonds *et al*, 2001; Yamada *et al*, 2002; Afshar-Kharghan *et al*, 2004). The first polymorphism is an amino acid dimorphism, Thr/Met, at residue 145 (Murata *et al*, 1992). The second polymorphism is a variable number tandem repeat [1–4 repeats (1R–4R)] of the 13-amino acid sequence, residues 399–411 (VNTR polymorphism) (Moroi *et al*, 1984; Ishida *et al*, 1991; Simsek *et al*, 1994). These two polymorphisms are in linkage disequilibrium (Ishida *et al*, 1991; Simsek *et al*, 1994). The ¹⁴⁵Met-allele, which is tightly linked to the 3R- or 4R-allele, is associated with increased risk. There is a race difference in the genotype distribution of the VNTR polymorphism; although 3R is observed in Caucasians, African-Americans (Afshar-Kharghan *et al*, 2004), Japanese, and Koreans (Ishida *et al*, 1996), 4R is observed in Japanese and Koreans (Ishida *et al*, 1996). Epidemiologic data indicate

that GPIIb α polymorphisms are clinically significant. Molecular mechanisms for the association between thrombus formation and those polymorphisms, however, are not yet clearly understood. To elucidate the effects of ¹⁴⁵Thr/Met and/or VNTR polymorphisms on interactions with VWF, we performed two series of experiments; (a) ristocetin-induced ¹²⁵I-labelled VWF binding to two recombinant fragments containing a partial GPIIb α sequence (¹His-³⁰²Ala) with either ¹⁴⁵Thr (145T) or ¹⁴⁵Met (145M), and (b) the interaction between immobilized VWF and four types of Chinese hamster ovary (CHO) cells expressing full-length GPIIb α / β /IX, ¹⁴⁵Thr/1R (T1R), ¹⁴⁵Met/1R (M1R), ¹⁴⁵Thr/4R (T4R), or ¹⁴⁵Met/4R (M4R), under flow conditions.

Methods

Preparation of recombinant GPIIb α fragments

The GPIIb α insert of a pBluescript KS (-) construct, which contained a cDNA encoding a partial GPIIb α sequence (¹His-³⁰²Ala) with ¹⁴⁵Thr, was cloned (Murata *et al*, 1991). The ¹⁴⁵Thr/Met substitutions on the GPIIb α insert were performed using Quick ChangeTM (Stratagene, La Jolla, CA, USA), and each insert was ligated with an expression vector pcDNA3.1Zeo (-) (Invitrogen, Groningen, The Netherlands). Each construct was sequenced to ensure that the introduced mutation was restricted to residue 145 and then transfected into CHO cells (Dainippon Pharmaceutical Co., Osaka, Japan) using FuGENETM 6 Transfection Reagent (Roche, Nutley, NJ, USA). Cells were cultured in the presence of 300 μ g/ml of zeocine (Invitrogen) for selection of stable transfectants. Culture medium containing secreted soluble protein was collected from 145T-, 145M-, or mock-transfected cells after serum-free culture medium for 48 h.

Quantitation and immunologic evaluation of recombinant proteins

The expression of each recombinant protein was confirmed by Western blot analysis with anti-GPIIb α monoclonal antibody, LJ-Ib α 1 (a generous gift from Dr Z.M. Ruggeri, The Scripps Research Institute, La Jolla, CA, USA), which recognizes an epitope within the 45-kDa domain and reacts strongly with the reduced GPIIb α fragment, using an enhanced chemiluminescence (ECL) Western blotting systemTM (Amersham Pharmacia Biotech, Buckinghamshire, UK). The amounts were measured by dot-blot analysis with LJ-Ib α 1 and ¹²⁵I-anti-mouse IgG (Daiichi Pure Chemicals, Tokyo, Japan). Purified recombinant GPIIb α (Moriki *et al*, 1997) was used as a standard. Equivalent amounts of 145T and 145M were evaluated for their immunologic reactivity toward a panel of anti-GPIIb α monoclonal antibodies, LJ-P3 (a generous gift of Dr Z.M. Ruggeri, The Scripps Research Institute), GUR83-35 (Takara Shuzo, Shiga, Japan), and GUR20-5 (Takara Shuzo), which recognize conformation-specific epitopes within the

45-kDa domain (Handa *et al*, 1986; Vicente *et al*, 1988; Kawasaki *et al*, 1995; Ikeda *et al*, 2000). ¹²⁵I-anti-mouse IgG was used as a secondary antibody in this quantitative analysis. A constant concentration (2 ng/ μ l) of 145T and 145M was used for subsequent functional analysis.

Ristocetin-induced ¹²⁵I-VWF binding to immobilized recombinant GPIIb α fragment

Human VWF was provided by WelFide Co. (Osaka, Japan), and was radiolabelled with ¹²⁵I (Amersham Pharmacia Biotech) according to the IODO-GEN procedure (Fraker & Speck, 1978). The analysis of ristocetin (final concentration, 1.0 mg/ml)-induced ¹²⁵I-labelled soluble VWF (final concentration, 1.0 μ g/ml) binding to immobilized 145T or 145M (400 ng/spot) was performed using the enzyme-linked immunofiltration assay apparatus (Pierce Chemical Co., Rockford, IL, USA). Details of this assay were described previously (Murata *et al*, 1991; Moriki *et al*, 1997). In the Scatchard plot analysis for the binding of ¹²⁵I-VWF (0.5–16 μ g/ml) to 145T or 145M, the dissociation constant was analysed by a simple regression model. It was assumed that the same proportion of VWF multimers binds to each recombinant protein, and that the molecular weight of VWF was 220-kDa.

Establishment of CHO cells expressing the GPIIb α β IX complex

A stable transfectant for GPIIb α β IX-expressing CHO cells was established, as described previously (Suzuki *et al*, 1999). A cDNA encoding the GPIIb α sequence was cloned into a pBluescript KS (-) as described previously (Suzuki *et al*, 1999) and was subcloned into a mammalian expression vector pcDNA 3.1 Hygro (+) (Invitrogen) using the restriction sites for Kpn I (Takara Shuzo) and Not I. We prepared four types of plasmids for expression, T1R, M1R, T4R, and M4R. ¹⁴⁵Thr/Met substitution was created by polymerase chain reaction (PCR)-based site-directed mutagenesis using Quick ChangeTM (Stratagene), and then inserted into the 1R or 4R sequences; PCR was performed on genomic DNA with the 1R and 4R alleles, followed by subcloning using a TA cloning kit (Invitrogen). Each insert was subsequently cloned into the GPIIb α -pcDNA 3.1 Hygro (+) using Xba I restriction sites and sequenced. Each plasmid was transfected into GPIIb α β IX-expressing CHO cells using FuGENETM 6. These cells were grown in culture medium with 800 μ g/ml of G418, 300 μ g/ml of zeocine, and 400 μ g/ml of hygromycin for selection of GPIIX, GPIIb β , and GPIIb α respectively.

Measurement for GPIIb α β IX expression on CHO cells

Expression of GPIIb α on CHO cells was confirmed by flowcytometry analysis with either the anti-GPIIb α antibody, LJ-P3, or the anti-GPIIX antibody, SZ1 (Immunotech,

Marseille, France), which reacts with the GPIbIX complex, but does not react with GPIb or GPIX alone. Four types of cells were independently sorted by fluorescence activated cell sorter (FACS) analysis using SZ1. Subsequently, quantitation of GPIb α on each cell was performed using an enzyme immuno-sorbent assay (EIA) with a glycolallicine EIA kit using GUR83–35 and GUR20–5, according to the supplied protocol. Purified glycolallicine of GPIb α (Lopez, 1994), which has a GPIb α extracytoplasmic domain that contains sites for the ¹⁴⁵Thr/Met and VNTR polymorphisms, was used as a standard in this assay.

Perfusion studies: analyses for the interaction of GPIb α IX-expressing CHO cells with immobilized VWF under flow conditions

Glass cover slips were incubated with 10 μ g/ml of VWF at 4°C overnight and then blocked with 0.5% bovine serum albumin (BSA) (Sigma-Aldrich, Tokyo, Japan) at room temperature for 1 h. CHO cells were harvested with 0.5 mmol/l EDTA, washed twice with phosphate buffered saline, and resuspended in 0.5 mmol/l EDTA/HEPES-Tyrode's buffer without Ca²⁺ and Mg²⁺ to a final concentration of 2 \times 10⁵/ml. The interaction between 10⁶ cells expressing GPIb α IX and immobilized VWF was examined using a recirculating flow chamber system (Nishiya *et al.*, 2000). Cells interacting with the surface were monitored for a 4-min period. Data were stored on video tape. Single-frame video images were analysed using an image processor, an Argus 50 image processor (Hamamatsu Photonics, Hamamatsu, Japan), and rolling velocities of the cells were analysed using an image processor, an Argus 20 image processor (Hamamatsu Photonics). Rolling velocity was determined as the distance cells rolled per second. To confirm the specificity of the cell rolling, experiments under flow conditions were performed in the presence of 10 μ g/ml of soluble-VWF or after incubation with 50 μ g/ml of anti-GPIb α antibody GUR83–35 at room temperature for 15 min.

Statistics

Differences in immunologic reactivity between 145T and 145M were assessed using Student's *t*-test. Analysis of covariance (ANCOVA) was used to compare the influence of three variables, GPIb α sequence (145T vs. 145M), VWF binding, and day of the experiment, in VWF binding between 145T and 145M. Analysis of variance (ANOVA) was used for analysis of GPIb α expression on CHO cells and the perfusion studies among four types of GPIb α -expressing cells. The Bonferroni *post hoc* test for multiple comparisons was performed to compare the rolling velocity among the cells. ANCOVA was used to analyse three variables; GPIb α sequence (T1R vs M4R), rolling velocity, and day of experiment. A *P*-value of less than 0.05 was considered to be statistically significant.

Results

Comparison of immunologic reactivity of recombinant GPIb α fragments

To characterize the ¹⁴⁵Thr/Met polymorphism, we established stable cell lines that secreted recombinant GPIb α fragments (¹His–³⁰²Ala), 145T or 145M, into the culture medium. The secretion of each fragment into the culture medium was confirmed by Western blot analysis using the LJ-Ib α 1 antibody under reduced conditions. An LJ-Ib α 1-positive species with a molecular mass of approximately 45-kDa was observed in 145T and 145M, but not in the culture medium from mock-transfected cells. Subsequently, we quantified each fragment by dot-blot analysis with LJ-Ib α 1 under reduced conditions. There was similar immunologic reactivity to LJ-Ib α 1 between 145T and 145M. An equivalent amount of each fragment was tested in dot-blot analysis for their immunologic reactivity to several anti-GPIb α monoclonal antibodies that recognize confirmation-specific epitopes within the 45-kDa domain and ¹²⁵I-anti mouse IgG as a secondary antibody. The binding of each antibody, as measured by counts per minute, was not significantly different between 145T and 145M (Table I), suggesting that the ¹⁴⁵Thr/Met polymorphism does not affect immunologic reactivity for LJ-P3, GUR20–5, and GUR83–35. Similar results by dot-blot analysis using the ECL detection system with anti-mouse IgG antibody as a secondary antibody were observed in seven independent experiments (data not shown).

Ristocetin-induced ¹²⁵I-labelled VWF binding to immobilized recombinant GPIb α fragments

To elucidate the effect of the ¹⁴⁵Thr/Met polymorphism on VWF binding, we performed an experiment using recombinant GPIb α fragments without the VNTR polymorphism site, containing residues 1–302. This binding was examined in the absence or presence of ristocetin under static conditions (Fig 1). The binding levels (pmol/well; mean \pm SD) were 0.011 \pm 0.005 for BSA, 0.018 \pm 0.008 for 145T, and 0.016 \pm 0.004 for 145M in the absence of ristocetin, indicating no specific binding in this experimental condition. In the presence of ristocetin, specific ¹²⁵I-VWF binding was observed in 145T and 145M, but not BSA; 0.015 \pm 0.008 for BSA, 0.039 \pm 0.015 for 145T, and

Table I. Immunologic reactivity (cpm count) in dot-blot analysis.

	145T	145M	<i>P</i> -value
LJ-Ib α 1	2594.0 \pm 17.0	2536.0 \pm 130.1	0.5957
LJ-P3	2532.0 \pm 93.3	2771.0 \pm 168.3	0.2211
GUR20–5	2777.0 \pm 75.0	2730.0 \pm 435.6	0.8943
GUR83–35	2930.0 \pm 45.3	2622.0 \pm 260.2	0.2409

Values are mean \pm SD of duplicate determinations in one experiment.

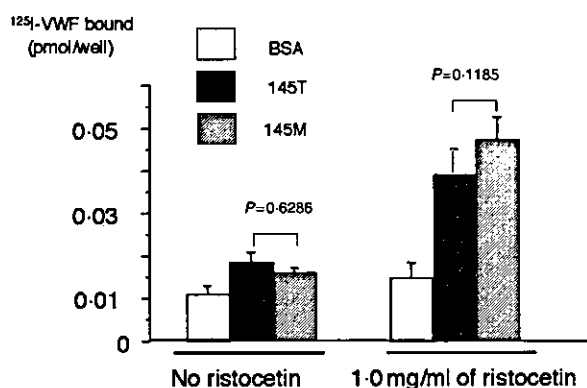


Fig 1. Binding of ristocetin-induced ^{125}I -labelled soluble VWF to immobilized recombinant GPIIb/IIIa fragment was analysed on nitrocellulose membrane. Membrane-bound radioactivity was counted to assess the binding. BSA was used as a control. Results are mean value \pm SD (pmol/well) of duplicates of three independent experiments. Error bars indicate SDs.

0.047 ± 0.017 for 145M, and the binding levels were not different between 145T and 145M ($P = 0.1185$).

To evaluate the binding affinities of 145T and 145M, a Scatchard plot analysis was performed in the presence of 1.0 mg/ml of ristocetin. Both samples had saturable binding of ^{125}I -VWF, and the dissociation constants (nmol/l; mean \pm SD) were 620.5 ± 176.1 for 145T and 406.0 ± 40.2 for 145M ($P = 0.0551$). The maximum number of binding sites (B_{max} , nmol/l; mean \pm SD) was 68.0 ± 11.4 for 145T and 56.1 ± 11.3 for 145M ($P = 0.1889$). These results suggest that 145T and 145M have a similar binding affinity for VWF in the presence of ristocetin.

Quantitation of GPIIb/IIIa expression on the GPIIb/IIIa-expressing CHO cells

We prepared four types of GPIIb/IIIa-expressing CHO cells; two naturally occurring sequences, T1R and M4R, and two artificial or extremely rare sequences, T4R and M1R, to investigate which GPIIb/IIIa polymorphisms affect the interaction with VWF under flow conditions. First, the surface density of the GPIIb/IIIa complex on each cell was examined by flowcytometry analysis with LJ-P3 or SZ-1, and the reactivity was not different among cells. Subsequently, four types of GPIIb/IIIa-expressing CHO cells were isolated using FACS to obtain cells with an equivalent amount of the GPIIb/IIIa complex on the surface. Moreover, quantitative determination of each sorted cell was performed by EIA using the anti-GPIIb/IIIa antibodies, GUR83-35 and GUR20-5. The GPIIb/IIIa expression levels, calculated by standard curves for absorbance and glycolaldehyde as a standard protein, are shown in Table II. There was no statistically significant difference in the GPIIb/IIIa expression levels among the four types of cells, although T4R had a slightly higher expression level.

Table II. GPIIb/IIIa molecule on single CHO cell.

GPIIb/IIIa sequence	GPIIb/IIIa molecule ($\times 10^6$)	P-value
T1R	4.26 ± 0.31	0.1279
M1R	4.46 ± 0.34	
T4R	5.26 ± 0.48	
M4R	4.36 ± 0.17	

Values are mean \pm SD of duplicate determinations in three independent experiments.

Interaction between immobilized VWF and CHO cells expressing the GPIIb/IIIa complex under flow conditions

To determine the optimal shear condition, preliminary studies were performed using T1R cells to monitor the interaction between immobilized VWF and GPIIb/IIIa-expressing CHO cells. Rolling cells per unit area (mm^2) of VWF-immobilized glass were counted under various shear conditions. The number of rolling cells was 26.91, 16.34, 8.65, 0.96, and 0 for shear conditions of 32/s, 64/s, 114/s, 214/s, and 600/s respectively. In CHO cells without GPIIb/IIIa, the rolling cell number was 3.84, 0.96, 0, 0, and 0 for shear conditions of 32/s, 64/s, 114/s, 214/s, and 600/s respectively. We then examined the effect of the anti-GPIIb/IIIa antibody GUR83-35 on rolling cell number per minute and rolling velocity. Under a shear condition of 32/s, the number of rolling cells per minute was 14 and 16 in the absence and presence of GUR83-35 respectively. Under a shear condition of 114/s, the number was 134 and 41 in the absence and presence of GUR83-35 respectively. The rolling velocity under a shear condition of 32/s was similar between the two experimental conditions; 240.61 ± 67.49 ($\mu\text{m/s}$, mean \pm SD) in the absence of GUR83-35 and 291.98 ± 60.92 in the presence of GUR83-35. In contrast, the rolling velocity under a shear condition of 114/s was different in the absence and presence of GUR83-35; 704.74 ± 153.5 and 959.10 ± 172.1 respectively. These findings indicated that the observed interaction was specific for GPIIb/IIIa under a shear condition of 114/s, but not of 32/s. Thus, we adopted the shear condition of 114/s for the subsequent experiments.

As shown in Fig 2 and Table III, the rolling velocity of M4R under shear conditions of 114/s was significantly slower than that of T1R ($P = 0.00042$). The rolling velocities of M1R and T4R were similar, with values that were intermediate between those for T1R and M4R. Moreover, we analysed the rolling velocity between T1R and M4R by ANOVA to test whether the difference identified by ANOVA was affected by different day of experiment. The rolling velocity was 1077.7 ± 20.9 (mean \pm SD) for T1R and 918.4 ± 17.3 for M4R ($P < 0.0001$), indicating that the significant difference between T1R and M4R was not influenced by interactions with other variables among the four independent experiments. The number of rolling cells interacting with the immobilized VWF per minute was 32.0 ± 5.6 for T1R, 34.7 ± 2.1 for M1R, 26.7 ± 3.1 for T4R, and 35.7 ± 2.5 for M4R. These values were not significantly different among the four types of cells